# Transgenic ablation of doublecortin-expressing cells suppresses adult neurogenesis and worsens stroke outcome in mice

**Kunlin Jin, Xiaomei Wang, Lin Xie, Xiao Ou Mao, and David A. Greenberg[1]**

Buck Institute for Age Research, Novato, CA 94945

Edited* by Solomon Snyder, Johns Hopkins University School of Medicine, Baltimore, MD, and approved March 22, 2010 (received for review January 6, 2010)

**Injury stimulates neurogenesis in the adult brain, but the role of injury-induced neurogenesis in brain repair and recovery is uncertain. One strategy for investigating this issue is to ablate neuronal precursors and thereby prevent neurogenesis, but this is difficult to achieve in a specific fashion. We produced transgenic mice that express herpes simplex virus thymidine kinase (TK) under control of the promoter for doublecortin (Dcx), a microtubule-associated protein expressed in newborn and migrating neurons. Treatment for 14 days with the antiviral drug ganciclovir (GCV) depleted Dcx-expressing and BrdU-labeled cells from the rostral subventricular zone and dentate gyrus, and abolished neurogenesis and associated neuromigration induced by focal cerebral ischemia. GCV treatment of Dcx-TK transgenic, but not WT, mice also increased infarct size and exacerbated postischemic sensorimotor behavioral deficits measured by rotarod, limb placing, and elevated body swing tests. These findings provide evidence that injury-induced neurogenesis contributes to stroke outcome and might therefore be a target for stroke therapy.**

The finding that brain injury stimulates the production of new neurons (neurogenesis) in the mammalian brain (1) suggests a role for this process in brain repair. Injury-induced neurogenesis is observed across a broad range of injury models in experimental animals and human patients. Focal brain ischemia, for example, triggers increased proliferation of neuronal precursor cells in the anterior subventricular zone (SVZ), followed by their migration into ischemic brain regions, where they differentiate and mature (2–6). This raises the possibility that therapeutic enhancement of injury-induced neurogenesis might constitute a new approach to the treatment of stroke or related disorders.

One strategy for investigating the contribution of adult neurogenesis to brain function or repair is to ablate neuronal precursors in the brain's principal neuroproliferative zones—the anterior SVZ and the hippocampal dentate gyrus (DG). Several techniques have been used for this purpose, including x-irradiation (7–13), antimitotic (4, 14–18) or other antiproliferative (19) drugs, and conditional transgenic targeting of selected [glial fibrillary acidic protein (GFAP)-, nestin-, or homolog of *Drosophila* tailless–expressing] cell populations with HSV-1 thymidine kinase (TK) (20–23) or inducible recombination (24). However, studies that use these ablation techniques to assess the functional significance of neurogenesis can be difficult to interpret, because ablation may be accompanied by inflammatory responses with microglial activation (7), alterations in microvascular anatomy (7), systemic toxicity (18), or involvement of nonneuronal cell lineages (25).

We report the results of studies on the effects of neuronal precursor cell depletion on outcome from experimental stroke in transgenic mice that express TK under control of the doublecortin (Dcx) promoter (26). Dcx is a microtubule-associated protein expressed primarily in migrating neurons during development (27, 28) and adulthood (29, 30), including injury-induced (31) neurogenesis. Because Dcx is a more specific marker of neuronal lineage than GFAP or nestin, and because Dcx is first expressed in close temporal relation to cell division (i.e., BrdU labeling) (29), we considered it a promising candidate gene target for TK ablation-based studies of the role of adult neurogenesis in determining outcome from experimental stroke.

## Results

**Generation of Dcx-TK Mice.** A 3.5-kb fragment upstream of the ATG start codon of Dcx is sufficient to drive the expression of reporter genes in embryonic and adult neuronal precursors (26). Transient transfection of mouse embryonic fibroblasts with this fragment leads to immunohistochemically detectable expression of Dcx and other neuronal (βIII-tubulin, microtubule-associated protein 2) but not astroglial (GFAP) or oligodendroglial (galactosylceramidase) lineage markers (26). Eight transgenic pDcx-TK founders (F0) were bred to F1. Three of these lines expressed TK in cells of adult brain SVZ and DG, indicating that the Dcx promoter we used can drive TK expression. The mice appeared healthy with normal growth and reproduction, and with basal levels of Dcx protein expression similar to those in WT mice (Fig. 1*A*).

**Neurogenesis in Dcx-TK Mice.** Brains from both WT and Dcx-TK transgenic mice not given ganciclovir (GCV) showed abundant expression of Dcx in DG subgranular zone and SVZ (Fig. 1*B*). Double-label immunohistochemistry of sections through the SVZ of Dcx-TK transgenic mice showed that TK was localized to nuclei of cells that expressed Dcx in the cytoplasm (Fig. 1*C*).

In preliminary experiments, WT and Dcx-TK mice were treated with saline or GCV for 14 days by the i.p. route. No GCV-induced change in food or water intake, overall health, or mortality was observed in either group, but body weight in Dcx-TK mice was ≈10% lower than that in WT mice at the conclusion of treatment. Therefore, the intracerebroventricular route was used to administer GCV in subsequent experiments, including all those reported here. GCV caused no change in the extent of Dcx expression or BrdU uptake in the SVZ of WT mice. In contrast, GCV-treated Dcx-TK mice exhibited profound depletion of Dcx-immunoreactive cells from SVZ (Fig. 1*D*). Depletion of Dcx-positive cells from SVZ of GCV-treated Dcx-TK mice was accompanied by a similar reduction in the number of cells that incorporated BrdU. Triple-label immunohistochemistry confirmed that despite almost complete disappearance of Dcx- and BrdU-positive cells from the SVZ of Dcx-TK transgenic mice, there was no loss of GFAP-expressing (astrocytic) cells (Fig. 1*E*). In addition, there was no evidence of microglial activation in GCV-treated mice that might indicate inflammation associated with secondary injury (Fig. 1*F*). These findings are consistent with the absence of a cytotoxic bystander effect of GCV on other cell types in this study.

Author contributions: K.J. and D.A.G. designed research; K.J., X.W., L.X., and X.M. performed research; K.J., X.W., L.X., X.M., and D.A.G. analyzed data; and K.J. and D.A.G. wrote the paper.

The authors declare no conflict of interest.

*This Direct Submission article had a prearranged editor.

[1]To whom correspondence should be addressed. E-mail: dgreenberg@buckinstitute.org.

This article contains supporting information online at www.pnas.org/cgi/content/full/1000154107/DCSupplemental.

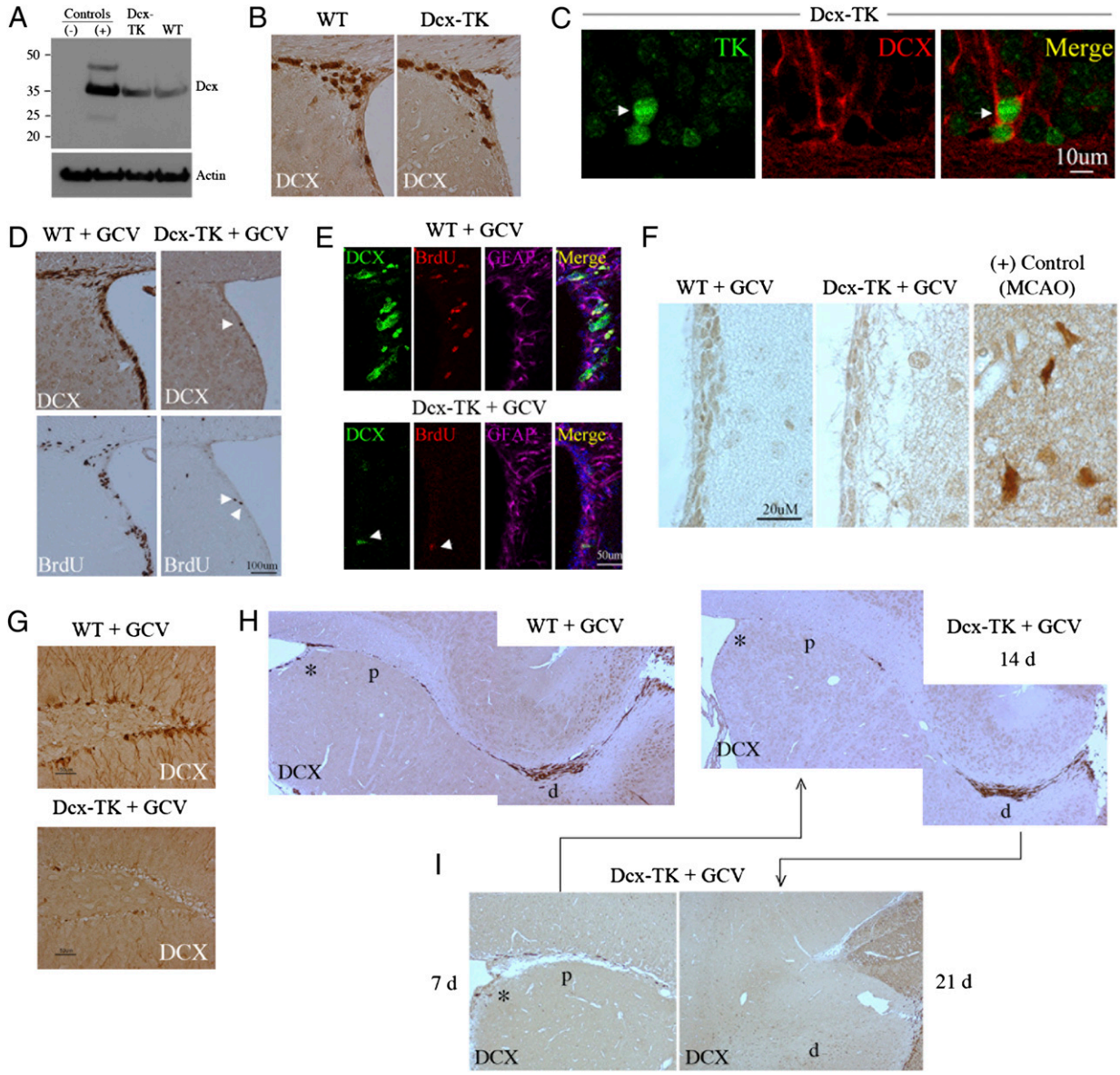


**Fig. 1.** Neurogenesis in Dcx-TK mice. (*A*) Dcx protein expression in Dcx-TK transgenic compared with WT mouse SVZ, with negative (ES cell–derived neuroepithelial precursors) and positive (E15 mouse brain) controls. (*B*) Dcx expression (brown) in SVZ of WT and Dcx-TK transgenic mice not treated with GCV. (*C*) Localization of nuclear TK expression (green, arrow) to cells expressing cytoplasmic Dcx (red) in SVZ of Dcx-TK transgenic mice not treated with GCV. (*D*) Depletion of Dcx- (top, brown) and BrdU- (bottom, brown) immunoreactive cells from SVZ of Dcx-TK but not WT mice treated for 14 days with GCV. Arrows indicate few remaining Dcx- and BrdU-immunopositive cells in GCV-treated Dcx-TK mice. (*E*) Sparing of GFAP- (purple) in contrast to Dcx- (green) and BrdU- (red) expressing cells in SVZ of Dcx-TK mice treated for 14 days with GCV; all three markers are spared in WT mice. Arrows indicate a rare Dcx- and BrdU-immunopositive cell. (*F*) Absence of microglial activation (Ox42 antibody staining, brown) in SVZ of GCV-treated WT and Dcx-TK mice, compared with a positive control (mouse cerebral cortex after MCAO). (*G*) Depletion of Dcx-immunoreactive cells (brown) from DG of Dcx-TK but not WT mice treated for 14 days with GCV. (*H*) Depletion of Dcx-immunoreactive cells (brown) from SVZ (*) and proximal (p) but not distal (d) RMS of Dcx-TK but not WT mice treated for 14 days with GCV. (*I*) Compared with Dcx-TK mice treated with GCV for 14 days, mice treated for 7 days showed relative preservation of Dcx-immunoreactive cells in SVZ (*) and proximal RMS (p), whereas mice treated for 21 days showed depletion of Dcx-immunoreactive cells in distal RMS (d).

GCV treatment for 14 days also depleted Dcx-positive cells from DG (Fig. 1*G*) and from the proximal but not distal rostral migratory stream (RMS) (Fig. 1*H*), through which new neurons normally migrate from SVZ to reach the olfactory bulb. When GCV was given for 7 instead of 14 days, many Dcx-positive cells persisted in the SVZ and proximal RMS, whereas after treatment for 28 days, Dcx-positive cells were eliminated from these areas and from the distal RMS as well (Fig. 1*I*). This time-dependent, proximodistal depletion of Dcx-expressing cells is consistent with the time course over which dividing neuronal precursors traverse the RMS (32) and suggests that Dcx-positive cells in the distal RMS of GCV-treated Dcx-TK mice represent cells that had completed division before GCV treatment began. Overall, these results indicate that Dcx-expressing neuronal precursor cells are severely depleted in neuroproliferative zones of the adult brain in GCV-treated Dcx-TK mice.

**Focal Cerebral Ischemia in Dcx-TK Mice.** Focal cerebral ischemia was induced by middle cerebral artery occlusion (MCAO) in Dcx-TK mice on day 14 of vehicle (saline) or GCV treatment. Administration of saline or GCV was then continued for an additional 24 h, at which time mice underwent sensorimotor testing and were then

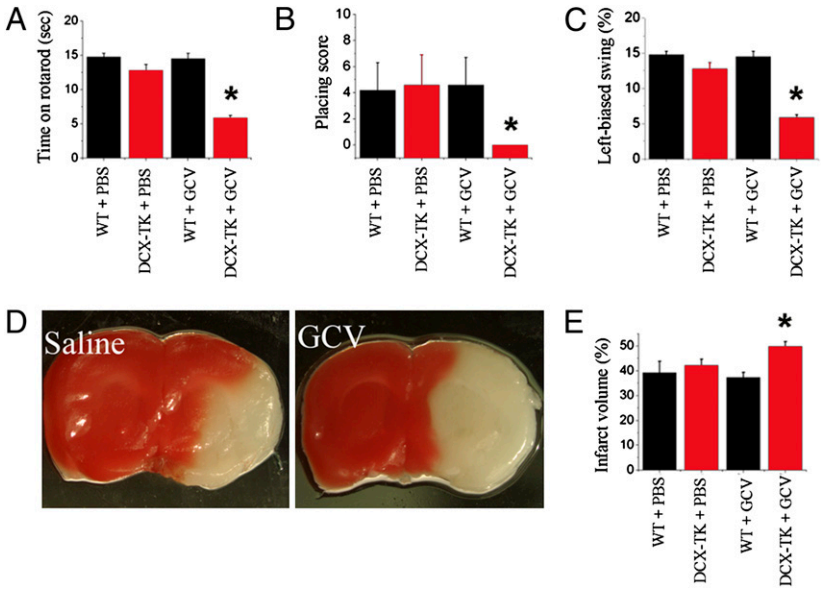


**Fig. 2.** Focal cerebral ischemia in Dcx-TK mice. WT (black bars) and Dcx-TK transgenic (DCX-TK, red bars) mice were treated for 14 days with saline vehicle (PBS) or GCV, then underwent MCAO to induce focal cerebral ischemia. Twenty-four hours later, behavioral testing was performed and mice were killed for measurement of infarct size. (*A*) Rotarod scores, expressed as time (s) mice remained on the rod; lower scores represent more severe deficits. (*B*) Limb-placing test scores, expressed according to the scale described in *Materials and Methods*; lower scores represent more severe deficits. (*C*) Elevated body swing test scores, expressed as percentage turns away from the ischemic hemisphere, as described in *Materials and Methods*; lower scores represent more severe deficits. (*D*) Infarct areas (white) in TTC- (red) stained coronal brain sections from PBS- and GCV-treated Dcx-TK mice. (*E*) Infarct volumes (expressed as percentage hemispheric volume) in PBS- and GCV- treated WT (black) and Dcx-TK (red) mice. $*P < 0.05$.

killed. Postischemic functional deficits, measured using the rotarod (Fig. 2*A*), limb placing (Fig. 2*B*), and elevated body swing (Fig. 2*C*) tests, were greater in GCV-treated Dcx-TK than in saline-treated Dcx-TK or saline- or GCV-treated WT mice. Histologic outcome was assessed by measuring infarct size, as determined by 2,3,5-triphenyltetrazolium hydrochloride (TTC) staining of coronal brain slices to determine infarct area (33), and then integrating area throughout the rostrocaudal extent of the infarct to calculate infarct volume (34). GCV treatment of Dcx-TK mice extended the area of infarction (Fig. 2*D*) and increased infarct volume compared with that observed after saline treatment of Dcx-TK or saline or GCV treatment of WT mice (Fig. 2*E*). This increase in infarct volume was not attributable to differences in brain edema, because the method used to determine infarct volume controls for differences in edema (34) and because whole wet brain weight after MCAO was not significantly different across treatment groups (PBS-treated WT, 505 ± 9 mg; GCV-treated WT, 501 ± 11 mg; PBS-treated Dcx-TK, 505 ± 11 mg; GCV-treated Dcx-TK, 513 ± 8 mg; $n = 3$–4 per group). Therefore, both neurobehavioral and histologic outcome from focal cerebral ischemia are adversely affected by ablation of Dcx-expressing cells.

**Ischemia-Induced Neurogenesis and Neuromigration in Dcx-TK Mice.** Ischemia-induced proliferation of neuronal precursors in SVZ is followed by migration of newborn neurons into the adjacent ischemic striatum (3–6). In WT mice that underwent MCAO, this was evidenced by an increase in the number of Dcx-positive cells in the ipsilateral SVZ, and the appearance of Dcx-positive cells, some with sterotypic migratory morphology (35), in the peri-infarct region of the striatum (Fig. 3*A*). A similar picture was observed ipsilateral but not contralateral to MCAO in Dcx-TK mice not given GCV (Fig. 3*B*). However, in GCV-treated Dcx-TK mice, in addition to the depletion of Dcx-positive cells from the SVZ noted above, Dcx-positive cells were absent from the striatum (Fig. 3*C*). Thus, GCV treatment ablated not only baseline, but also ischemia-induced neurogenesis and subsequent neuromigration in Dcx-TK mice.

## Discussion

A small number of studies have used ablation techniques to study neurogenesis in experimental stroke. Arvidsson et al. (4) administered cytosine-β-D-arabinofuranoside (Ara-C) to mice for 12 days after transient MCAO and found that it reduced the number of BrdU-positive cells in the ipsilateral SVZ and the density of BrdU/Dcx-positive cells in the ischemic striatum by ≈90%. Zhang et al. (16) treated mice with Ara-C for 7 days after MCAO and found similar reductions in the number of BrdU-positive cells in the ipsilateral SVZ and BrdU/Dcx-positive cells in the ischemic striatum. However, neither of these studies examined the effect of Ara-C on histologic or functional outcome from stroke. Raber et al. (10) treated gerbils with cranial x-irradiation 2 weeks before the induction of global cerebral ischemia by bilateral common carotid artery occlusion. Irradiation reduced the number of BrdU-positive cells in the DG granule cell layer by >75% and the number of BrdU/βIII-tubulin-positive cells by >85%, compared with counts in nonirradiated ischemic animals. Preischemic irradiation also worsened performance in a water-maze task, indicating exacerbation of ischemia-induced deficits in spatial learning.

In an effort to more precisely ablate specific populations of neural precursor cells, some studies have made use of conditional TK-expressing transgenic mouse strains. Expression of TK renders the cell population of interest susceptible to the cytotoxic effect of GCV (36). Studies to date have used either GFAP (20–22) or nestin (23) to direct the expression of TK. GFAP is a type III intermediate filament protein expressed classically in astrocytes, including SVZ astrocytes that give rise to neurons (37) and oligodendrocytes (38). Nestin is a type VI intermediate filament protein associated with cells of neuroepithelial origin, including both neuronal and astroglial lineages, as well as a variety of non-neural cell types (39).

Imura et al. (20) found that GCV treatment of astrocyte cultures from postnatal GFAP-TK transgenic mice, or systemic administration of GCV to adult GFAP-TK mice, prevented the growth of multilineage neurosphere cultures in vitro. The same group

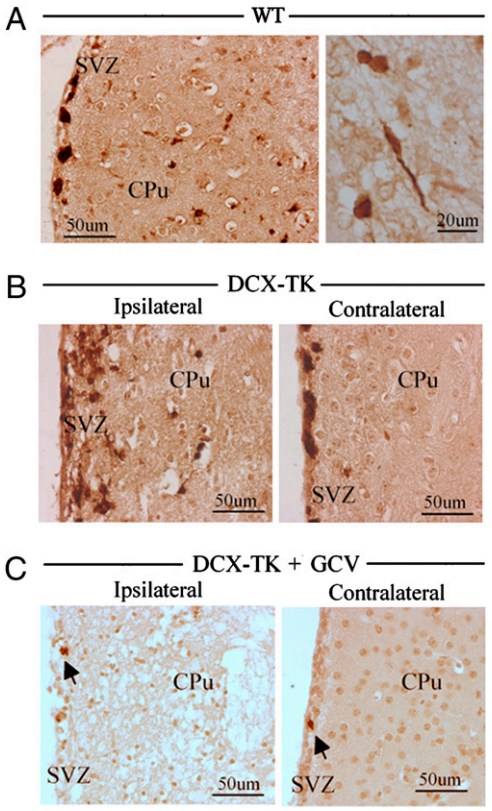


**Fig. 3.** Ischemia-induced neurogenesis and neuromigration in Dcx-TK mice. (*A*) Dcx expression (brown) in SVZ and adjacent periinfarct striatum (CPu) of WT mice 24 h after MCAO. (*Right*) Higher-magnification view showing Dcx-expressing cells with migratory morphology in periinfarct striatum. (*B*) Dcx expression (brown) in SVZ and adjacent striatum (CPu) ipsilateral and contralateral to infarct, in PBS-treated Dcx-TK mice 24 h after MCAO. (*C*) Dcx expression (brown) in SVZ and adjacent striatum (CPu) ipsilateral and contralateral to infarct, in GCV-treated Dcx-TK mice 24 h after MCAO.

showed subsequently that treating GFAP-TK mice for 20 days with GCV reduced the number of BrdU-positive cells by ≈70% in the DG subgranular zone and by ≈80% in the SVZ, and also depleted cells in these regions that expressed embryonic nerve-cell adhesion molecule (22). Morshead et al. (21) reported similar findings. Finally, Singer et al. (23) treated nestin-TK mice for 28 days with intracerebroventricular GCV, which caused near-complete loss of dividing (Mcm2- or Ki67-positive) cells and of Dcx-positive cells from both DG and SVZ. None of these studies examined behavioral consequences of cell depletion nor effects on recovery from ischemia or other forms of brain injury.

Our results indicate that SVZ neurogenesis contributes to short-term functional outcome after experimental stroke in mice. This conclusion is based on the finding that ablation of Dcx-expressing cells with GCV before MCAO in Dcx-TK transgenic mice results in increased infarct size and more severe neurologic deficits. These results are consistent with those of the one previous study in which neurogenesis was ablated and an adverse effect on outcome from cerebral ischemia was observed (10). That study differed from ours in that x-irradiation was used to inhibit neurogenesis, the model used was global rather than focal ischemia (stroke), and histologic outcome was not studied. We chose to target Dcx-expressing cells because we expected that this approach would be more specific for neuronal precursors than radiation or drugs, which can affect dividing cells irrespective of cell lineage, or GFAP- or nestin-based ablation, because these markers are also expressed in nonneuronal cells (37–39). Dcx expression has been reported in some phenotypically mature neurons of the rat hippocampus, striatum, olfactory bulb, and piriform cortex (40), but the cytotoxic effect of GCV depends on DNA replication, so nondividing cells are spared (36). A subpopulation of multipotent, neurosphere-forming cells that express low levels of Dcx has also been described (41). Finally, Dcx-immunopositive cells with morphologic features of mature astrocytes have been reported in human brain autopsy specimens and a human glioblastoma cell line (42) but not in rodent brain.

The finding that ablation of neurogenesis worsens outcome from MCAO suggests that neurogenesis normally exerts a salutary influence in this setting. However, the effect that we observed occurred too early to be explained by a failure to produce new mature neurons, which requires weeks rather than days (4). Therefore, the beneficial effect of neurogenesis on early outcome after ischemia is likely mediated by other than neuronal replacement. Neuroprotective effects of immature neurons have been proposed previously and have been ascribed to the release of chemical mediators (43). Certain growth factors, such as VEGF, also improve early postischemic endpoints, such as infarct size, too quickly for their effects to be explained by the production of mature new neurons (44). In fact, secretion of VEGF has been implicated in the beneficial effect of marrow stromal cells administered after ischemia (45).

In conclusion, ischemia-induced neurogenesis seems to help mitigate histologic and neurobehavioral deficits in the early aftermath of experimental stroke. This effect occurs too soon to be accounted for by the de novo production of fully differentiated neurons, although such neurons do seem to be produced later and to survive long term (46), and may contribute to recovery in the chronic phase of stroke. In the shorter term, neurogenesis may enhance brain repair through the release of growth factors or other soluble mediators. Clinical experience indicates that improvement after stroke may be observed early in the course but typically continues for several months (47). Accordingly, it would not be unexpected if multiple repair mechanisms, operating within different time frames, were to coexist.

## Materials and Methods

**Animals.** Dcx-TK transgenic mice were generated in the Buck Institute Transgenic Laboratory. To prepare the Dcx-TK transgene, mouse genomic DNA was isolated from embryonic brain, and PCR was performed using Dcx promoter-specific primers (sense, CTTTTGTCTCTCTCAGCCTC; antisense, AGAAAAGGGTGGAGATAAGG). These were designed based on the GeneBank database sequence (accession no. AY590498), which was further verified by DNA sequencing. The mouse Dcx promoter was directionally cloned into the plasmid. The HSV-TK gene was excised with BamHI from pBS mcs1mCMVTKpA vector and cloned in a plasmid containing the Dcx promoter. The pDcx-TK transgenic vector was injected into CD1 embryos. Identification and characterization of transgenic mouse lines was performed by PCR using HSV-TK-specific primers (HSVTK-1: 5′-CCACCACG CAACTGCTGGTG-3′; and HSVTK-2: 5′-CGAGG CGGTGTTGTGTGGTGT-3′). Mice were used in experiments at age 2 to 3 months. All procedures were approved by local committee review and conducted according to the National Institutes of Health (NIH) Guide for the Care and Use of Laboratory Animals, with an effort to minimize suffering and reduce animal numbers.

**GCV Administration.** In pilot studies, 30, 50, 75, or 100 mg/kg GCV (Cytovene, Roche) was administered daily via i.p. injection for 7, 14, or 21 days. However, regimens that produced depletion of Dcx-expressing cells (≥50 mg/kg for ≥14 days) caused weight loss of 10% or more in Dcx-TK transgenic mice. To avoid this and other possible systemic effects, in the experiments reported here, GCV was infused into the lateral ventricle using an osmotic minipump. Mice were anesthetized with 4% isoflurane in 70% $N_2O$/30% $O_2$, implanted with an osmotic minipumps (Alzet 1003D), and infused continuously for 14 days with 0.25 μL/h of either 20 mM GCV or normal saline. Focal ischemia was induced 14 days after the onset of GCV administration. Depletion of Dcx-expressing cells was confirmed by immunohistochemistry.

**BrdU Administration.** BrdU (50 mg/kg in saline; Sigma) was given by the i.p. route twice daily on the last day of GCV administration, and animals were killed 24 h

later. Brains were freshly isolated, and 50-μm coronal sections were cut with a cryostat and stored at −80 °C. Some brains were perfused with 0.9% saline and 4% paraformaldehyde in PBS (pH 7.4) and embedded in paraffin.

**Western Blotting.** The SVZ was dissected from mouse brains and cell lysates extracted in PBS containing 0.05% Nonidet P-40, 0.25% sodium deoxycholate, 50 mM Tris·HCl (pH 8.5), 100 mM NaCl, 1 mM EDTA (pH 8.0), 1 μg/mL aprotinin, and 100 μg/mL phenylmethylsulfonyl fluoride. Protein (50 μg, determined using a Bio-Rad assay) was boiled at 100 °C in SDS sample buffer for 5 min, electrophoresed on SDS/12% PAGE gels, and transferred to PVDF membranes, which were incubated overnight at 4 °C with rabbit polyclonal anti-DCX (1:1000; Santa Cruz Biotechnology), or mouse monoclonal anti-actin (1:20,000; Oncogene Science). Membranes were washed with PBS/0.1% Tween 20, incubated at room temperature for 60 min with HRP-conjugated anti-rabbit or anti-mouse secondary antibody (1:3,000; Santa Cruz Biotechnology) and washed three times for 15 min with PBS/Tween 20. Peroxidase activity was visualized by chemiluminescence (NEN Life Science Products). Antibodies were removed with stripping buffer (100 mM 2-mercaptoethanol/2% SDS/62.5 mM Tris·HCl, pH. 6.7) at 50 °C for 30 min, followed by washing with PBS/Tween 20 and reprobing.

**Immunohistochemistry.** Paraffin-embedded, 6-μm sections were deparaffinized with xylene and rehydrated with ethanol. To detect BrdU-labeled cells, sections were incubated in methanol at −20 °C for 10 min and in 2 M HCl at 37 °C for 50 min, and rinsed in 0.1 M boric acid (pH 8.5). Sections were then incubated in 1% $H_2O_2$ for 15 min and in blocking solution (2% goat serum, 0.3% Triton X-100, and 0.1% BSA in PBS) for 2 h at room temperature, before being treated with mouse monoclonal anti-BrdU overnight at 4 °C. Dcx immunohistochemistry was conducted using a standard protocol with antigen retrieval, according to the manufacturer's instructions (Vector Laboratories). The primary antibodies used were mouse monoclonal anti-BrdU (2 μg/mL; Roche), affinity-purified goat anti-Dcx (1:200; Santa Cruz Biotechnology), and mouse monoclonal OX42 (1:100; Sertotec). Sections were washed with PBS and incubated with biotinylated donkey anti-goat or biotinylated horse anti-mouse antibody (all 1:200; Santa Cruz Biotechnology) for 1 h at room temperature, then washed and placed in avidin–peroxidase conjugate solution (Vector Laboratories) for 1 h. The HRP reaction was detected with 0.05% diaminobenzidine and 0.03% $H_2O_2$. Processing was stopped with $H_2O$, and sections were dehydrated through graded alcohols, cleared in xylene, and coverslipped in permanent mounting medium (Vector Laboratories). Sections were examined with a Nikon E800 epifluorescence microscope. Controls included omitting the primary and secondary antibodies.

**Multilabel Immunohistochemistry.** Multilabel immunohistochemistry was performed as described elsewhere (6). The primary antibodies used, in addition to those listed above, were rabbit anti-GFAP (1:1,000; Sigma) and goat anti-HSV1 TK (vL-20; 1:200; Santa Cruz Biotechnology). Secondary antibodies were Alexa Fluor 488-, 594-, or 647-conjugated donkey anti-mouse, anti-goat, or anti-rabbit IgG (1:200–500; Molecular Probes). Fluorescence signals were detected using an LSM 510 NLO Confocal Scanning System mounted on an Axiovert 200 inverted microscope (Carl Zeiss) equipped with a two-photon Chameleon laser (Coherent), and images were acquired using LSM 510 Imaging Software (Carl Zeiss). Two- or three-color images were scanned using Ar, 543 HeNe, 633 HeNe, and Chameleon lasers. Selected images were viewed at high magnification. Controls included omitting either the primary or secondary antibody or preabsorbing the primary antibody.

**Focal Cerebral Ischemia.** Permanent MCAO was induced by intraluminal occlusion with a nylon monofilament suture. Male mice weighing 30–35 g were anesthetized with 2.0% isoflurane in 30% $O_2$ and 70% $N_2O$ using a vaporizer. Rectal temperature was maintained at 37 ± 0.5 °C with a thermostat-controlled heating blanket (Harvard Apparatus). Blood was analyzed using an ISTAT portable clinical analyzer and $EC8^+$ cartridge (Heska); results of pre- and post-MCAO arterial blood studies are shown in Table S1. After the neck was incised in the anterior midline, the left external carotid artery was exposed, ligated with a 6-0 silk suture, and dissected distally, and its branches were electrocoagulated; the left internal carotid artery was then isolated and separated from the vagus nerve. A 6-0 surgical monofilament nylon suture (Devis and Geck) was blunted at the end, introduced into the left internal carotid artery through the external carotid artery stump, and advanced 9 to 10 mm past the common carotid bifurcation. The skin was sutured within 10 min of incision. After recovery from anesthesia, mice were kept in a 20 °C air-conditioned room. Sham-operated rats underwent identical surgery except that the suture was not inserted.

**Rotarod Test.** Mice were trained on an accelerating (from 5 to 40 rpm) rotating rod (rotarod) for 3 days before MCAO; only those mice able to remain on the rod for 20 s at 40 rpm were subjected to MCAO (48). Test sessions consisting of three trials at 40 rpm were carried out just before MCAO and at 24 h after focal ischemia by an investigator who was blinded to the experimental groups. The final score was expressed as the mean time that a mouse was able to remain on the rod over three trials.

**Limb Placing Test.** Limb placing, a test of lateralized postischemic sensorimotor dysfunction (49), was evaluated bilaterally 24 h after ischemia. The test consisted of seven limb-placing tasks, which were scored by a blinded observer as follows: 0, no placing; 1, incomplete or delayed placing; 2, complete, immediate placing. Forelimb and hindlimb scores were averaged for each animal.

**Elevated Body Swing Test.** The elevated body swing test was used to test asymmetric motor behavior. Mice held by the base of the tail were raised ≈10 cm above the testing surface (50). The initial direction of body swing, constituting a turn of the upper body of >10° to either side, was recorded in three sets of 10 trials, performed over 5 min. The number of turns in each (left or right) direction was recorded, and the percentage of turns made to the side contralateral to the ischemic hemisphere (percent left-biased swing) was calculated. For each mouse, average scores were determined.

**Infarct Volume Measurement.** Mice were anesthetized and decapitated 24 h after the onset of ischemia. Brains were removed and 1-mm coronal sections immersed in 2% TTC in saline for 20 min at 37 °C, then fixed for 2 h in 4% paraformaldehyde (33). In some cases, infarct area was determined by hematoxylin and eosin staining. Infarct area, left hemisphere area, and total brain area were measured by a blinded observer using the NIH Image program, and areas were multiplied by the distance between sections to obtain the respective volumes. Infarct volume was calculated as a percentage of the volume of the contralateral hemisphere, as described previously (34).

**Statistical Analysis.** Behavioral testing was conducted using 12–16 mice and infarct volume was measured using 5–7 mice per group. Results are reported as mean ± SD. The significance of differences between means was assessed by Student *t* test (single comparisons) and ANOVA followed by Bonferroni post hoc or Fisher protected least significant difference (multiple comparisons), with $P < 0.05$ considered statistically significant.

**ACKNOWLEDGMENTS.** Supported by US Public Health Service Grants AG21980 and NS57186 (to K.J.) and NS44921 and NS62414 (to D.A.G.).

1. Gould E, Tanapat P (1997) Lesion-induced proliferation of neuronal progenitors in the dentate gyrus of the adult rat. *Neuroscience* 80:427–436.
2. Jin K, et al. (2001) Neurogenesis in dentate subgranular zone and rostral subventricular zone after focal cerebral ischemia in the rat. *Proc Natl Acad Sci USA* 98:4710–4715.
3. Zhang RL, Zhang ZG, Zhang L, Chopp M (2001) Proliferation and differentiation of progenitor cells in the cortex and the subventricular zone in the adult rat after focal cerebral ischemia. *Neuroscience* 105:33–41.
4. Arvidsson A, Collin T, Kirik D, Kokaia Z, Lindvall O (2002) Neuronal replacement from endogenous precursors in the adult brain after stroke. *Nat Med* 8:963–970.
5. Parent JM, Vexler ZS, Gong C, Derugin N, Ferriero DM (2002) Rat forebrain neurogenesis and striatal neuron replacement after focal stroke. *Ann Neurol* 52: 802–813.
6. Jin K, et al. (2003) Directed migration of neuronal precursors into the ischemic cerebral cortex and striatum. *Mol Cell Neurosci* 24:171–189.
7. Monje ML, Mizumatsu S, Fike JR, Palmer TD (2002) Irradiation induces neural precursor-cell dysfunction. *Nat Med* 8:955–962.
8. Mizumatsu S, et al. (2003) Extreme sensitivity of adult neurogenesis to low doses of X-irradiation. *Cancer Res* 63:4021–4027.
9. Santarelli L, et al. (2003) Requirement of hippocampal neurogenesis for the behavioral effects of antidepressants. *Science* 301:805–809.
10. Raber J, et al. (2004) Irradiation attenuates neurogenesis and exacerbates ischemia-induced deficits. *Ann Neurol* 55:381–389.
11. Fukuda A, et al. (2005) Age-dependent sensitivity of the developing brain to irradiation is correlated with the number and vulnerability of progenitor cells. *J Neurochem* 92:569–584.
12. Snyder JS, Hong NS, McDonald RJ, Wojtowicz JM (2005) A role for adult neurogenesis in spatial long-term memory. *Neuroscience* 130:843–852.
13. Clelland CD, et al. (2009) A functional role for adult hippocampal neurogenesis in spatial pattern separation. *Science* 325:210–213.

14. Doetsch F, García-Verdugo JM, Alvarez-Buylla A (1999) Regeneration of a germinal layer in the adult mammalian brain. *Proc Natl Acad Sci USA* 96:11619–11624.
15. Shors TJ, et al. (2001) Neurogenesis in the adult is involved in the formation of trace memories. *Nature* 410:372–376.
16. Zhang R, et al. (2004) Activated neural stem cells contribute to stroke-induced neurogenesis and neuroblast migration toward the infarct boundary in adult rats. *J Cereb Blood Flow Metab* 24:441–448.
17. Bruel-Jungerman E, Laroche S, Rampon C (2005) New neurons in the dentate gyrus are involved in the expression of enhanced long-term memory following environmental enrichment. *Eur J Neurosci* 21:513–521.
18. Dupret D, et al. (2005) Methylazoxymethanol acetate does not fully block cell genesis in the young and aged dentate gyrus. *Eur J Neurosci* 22:778–783.
19. Crandall J, et al. (2004) 13-cis-retinoic acid suppresses hippocampal cell division and hippocampal-dependent learning in mice. *Proc Natl Acad Sci USA* 101:5111–5116.
20. Imura T, Kornblum HI, Sofroniew MV (2003) The predominant neural stem cell isolated from postnatal and adult forebrain but not early embryonic forebrain expresses GFAP. *J Neurosci* 23:2824–2832.
21. Morshead CM, Garcia AD, Sofroniew MV, van Der Kooy D (2003) The ablation of glial fibrillary acidic protein-positive cells from the adult central nervous system results in the loss of forebrain neural stem cells but not retinal stem cells. *Eur J Neurosci* 18: 76–84.
22. Garcia AD, Doan NB, Imura T, Bush TG, Sofroniew MV (2004) GFAP-expressing progenitors are the principal source of constitutive neurogenesis in adult mouse forebrain. *Nat Neurosci* 7:1233–1241.
23. Singer BH, et al. (2009) Conditional ablation and recovery of forebrain neurogenesis in the mouse. *J Comp Neurol* 514:567–582.
24. Zhang CL, Zou Y, He W, Gage FH, Evans RM (2008) A role for adult TLX-positive neural stem cells in learning and behaviour. *Nature* 451:1004–1007.
25. Bush TG, et al. (1999) Leukocyte infiltration, neuronal degeneration, and neurite outgrowth after ablation of scar-forming, reactive astrocytes in adult transgenic mice. *Neuron* 23:297–308.
26. Karl C, et al. (2005) Neuronal precursor-specific activity of a human doublecortin regulatory sequence. *J Neurochem* 92:264–282.
27. Francis F, et al. (1999) Doublecortin is a developmentally regulated, microtubule-associated protein expressed in migrating and differentiating neurons. *Neuron* 23: 247–256.
28. Gleeson JG, Lin PT, Flanagan LA, Walsh CA (1999) Doublecortin is a microtubule-associated protein and is expressed widely by migrating neurons. *Neuron* 23:257–271.
29. Brown JP, et al. (2003) Transient expression of doublecortin during adult neurogenesis. *J Comp Neurol* 467:1–10.
30. Rao MS, Shetty AK (2004) Efficacy of doublecortin as a marker to analyse the absolute number and dendritic growth of newly generated neurons in the adult dentate gyrus. *Eur J Neurosci* 19:234–246.
31. Couillard-Despres S, et al. (2005) Doublecortin expression levels in adult brain reflect neurogenesis. *Eur J Neurosci* 21:1–14.
32. Okano HJ, Pfaff DW, Gibbs RB (1993) RB and Cdc2 expression in brain: Correlations with $^{3}$H-thymidine incorporation and neurogenesis. *J Neurosci* 13:2930–2938.
33. Bederson JB, et al. (1986) Evaluation of 2,3,5-triphenyltetrazolium chloride as a stain for detection and quantification of experimental cerebral infarction in rats. *Stroke* 17: 1304–1308.
34. Swanson RA, et al. (1990) A semiautomated method for measuring brain infarct volume. *J Cereb Blood Flow Metab* 10:290–293.
35. Nam SC, et al. (2007) Dynamic features of postnatal subventricular zone cell motility: A two-photon time-lapse study. *J Comp Neurol* 505:190–208.
36. Fillat C, Carrió M, Cascante A, Sangro B (2003) Suicide gene therapy mediated by the Herpes Simplex virus thymidine kinase gene/Ganciclovir system: Fifteen years of application. *Curr Gene Ther* 3:13–26.
37. Doetsch F, Caillé I, Lim DA, García-Verdugo JM, Alvarez-Buylla A (1999) Subventricular zone astrocytes are neural stem cells in the adult mammalian brain. *Cell* 97:703–716.
38. Menn B, et al. (2006) Origin of oligodendrocytes in the subventricular zone of the adult brain. *J Neurosci* 26:7907–7918.
39. Wiese C, et al. (2004) Nestin expression—a property of multi-lineage progenitor cells? *Cell Mol Life Sci* 61:2510–2522.
40. Nacher J, Crespo C, McEwen BS (2001) Doublecortin expression in the adult rat telencephalon. *Eur J Neurosci* 14:629–644.
41. Walker TL, Yasuda T, Adams DJ, Bartlett PF (2007) The doublecortin-expressing population in the developing and adult brain contains multipotential precursors in addition to neuronal-lineage cells. *J Neurosci* 27:3734–3742.
42. Verwer RW, et al. (2007) Mature astrocytes in the adult human neocortex express the early neuronal marker doublecortin. *Brain* 130:3321–3335.
43. Rafuse VF, Soundararajan P, Leopold C, Robertson HA (2005) Neuroprotective properties of cultured neural progenitor cells are associated with the production of sonic hedgehog. *Neuroscience* 131:899–916.
44. Sun Y, et al. (2003) VEGF-induced neuroprotection, neurogenesis, and angiogenesis after focal cerebral ischemia. *J Clin Invest* 111:1843–1851.
45. Chen J, et al. (2003) Intravenous administration of human bone marrow stromal cells induces angiogenesis in the ischemic boundary zone after stroke in rats. *Circ Res* 92: 692–699.
46. Thored P, et al. (2006) Persistent production of neurons from adult brain stem cells during recovery after stroke. *Stem Cells* 24:739–747.
47. Dobkin BH (2005) Clinical practice. Rehabilitation after stroke. *N Engl J Med* 352: 1677–1684.
48. Sugiura S, et al. (2005) Adenovirus-mediated gene transfer of heparin-binding epidermal growth factor-like growth factor enhances neurogenesis and angiogenesis after focal cerebral ischemia in rats. *Stroke* 36:859–864.
49. Jolkkonen J, et al. (2000) Behavioral effects of the alpha(2)-adrenoceptor antagonist, atipamezole, after focal cerebral ischemia in rats. *Eur J Pharmacol* 400:211–219.
50. Borlongan CV, Sanberg PR (1995) Elevated body swing test: A new behavioral parameter for rats with 6-hydroxydopamine-induced hemiparkinsonism. *J Neurosci* 15:5372–5378.